

Analysis and optimal design of fiber-reinforced composite structures: sail against the wind

R. Nascimbene*

EUCENTRE, Via Ferrata 1, Pavia, Italy

(Received January 31, 2012, Revised May 17, 2012, Accepted June 20, 2012)

Abstract. The aim of the paper is to use optimization and advanced numerical computation of a sail fiber-reinforced composite model to increase the performance of a yacht under wind action. Designing a composite-shell system against the wind is a very complex problem, which only in the last two decades has been approached by advanced modeling, optimization and computer fluid dynamics (CFDs) based methods. A sail is a tensile structure hoisted on the rig of a yacht, inflated by wind pressure. Our objective is the multiple criteria optimization of a sail, the engine of a yacht, in order to obtain the maximum thrust force for a given load distribution. We will compute the best possible yarn thickness orientation and distribution in order to minimize the total fiber volume with some displacement constraints and in order to leave the most uniform stress distribution over the whole structure. In this paper our attention will be focused on computer simulation, modeling and optimization of a sail-shape mathematical model in different regatta and wind conditions, with the purpose of improving maneuverability and speed made good.

Keywords: wind action; finite element analysis; sail; composites; fiber material

1. Introduction

The sail/hull research and fabrication have known a significant increase under the impulse of yacht racing such as the America's Cup, AEC Yacht Race, RORC and more. When looking at the performance in a sailing yacht design the first conceptual subdivision must be done between cruising yachts and racing yachts. We will focus on racing yachts particularly on sail designs that require advanced technologies in: optimization both geometrically (area, shape, fiber orientation) and mechanically (thickness, material layout, failure or strength criteria), advanced numerical modeling and fluid-structure interaction.

The design of a sailing yacht has evolved faster and faster in the last two decades along many development paths (Fallow 1996, Hedges *et al.* 1996, Parolini and Quarteroni 2005, Spalatel-Lazar 2008). It is a very complex problem, which involves three main steps: 1) preliminary design to determine, by CFDs as well as by naval architecture methods, the main ship's characteristics, such as: hull and sail shape, thrust as well as rudder selection, mast and boom length, material characteristics; 2) finite element modeling, discretization and optimization

* Corresponding author, Researcher, E-mail: roberto.nascimbene@eucentre.it

of the preliminary yacht and sail mathematical model in different regatta, wind and environmental conditions, with the purpose of evaluating maneuverability and performance (Parolini and Quarteroni 2005); 3) wind tunnel tests (Lasher *et al.* 2005).

In this paper the attention will be focused on point 2, where sail multiple criteria optimization problem (Moraes *et al.* 2007, Cinquini *et al.* 2001) is approached by a convex linearization optimization algorithm (Fleury 1989). The procedure presented in Fig. 1 is used to generate and evaluate a number of design tool and wind conditions to derive a sail that best fits a set of performance criteria. The main goal of the current research is to highlight the possibility of using analytical and numerical optimization algorithms coupled to advanced finite element analyses for determining sail shape and mechanical properties under specific wind conditions. Initially we consider a simplified two dimensional (2D) undeformed and unstressed rigid sail model to facilitate the development of the numerical optimization procedure (Part 1 in Fig. 1). Once the 2D model has been derived, a three dimensional (3D) flying-shape sail, to account for the elastic nature of the sail cloth, will be analyzed using a finite element procedure in order to find the best yarns distribution and orientation (Part 2 in Fig. 1) (Cheng and Kikuchi 1994, Pedersen 1989).

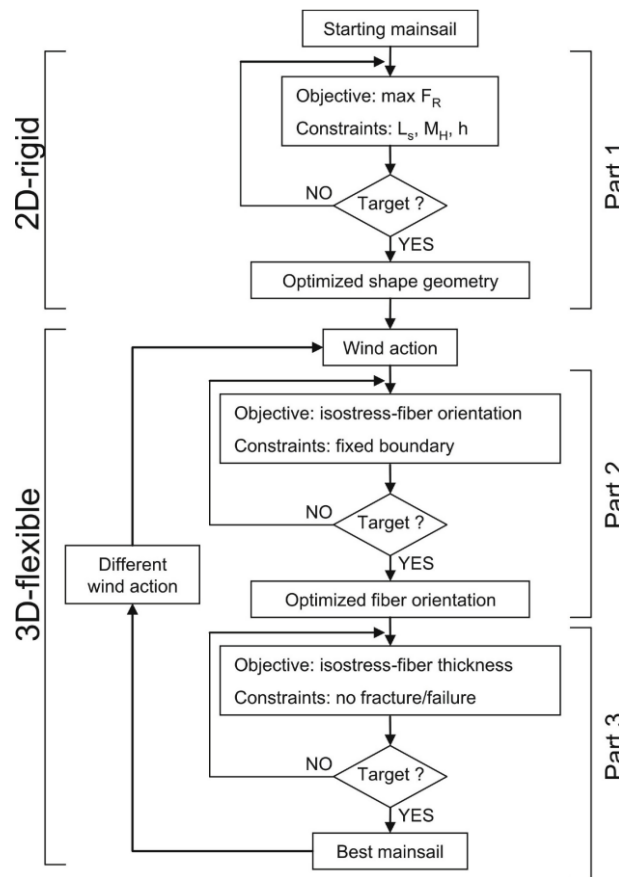


Fig. 1 Sail design and optimization process showing the relations between the main three parts of the research and the hypotheses, objectives and constraints of the numerical procedure implemented

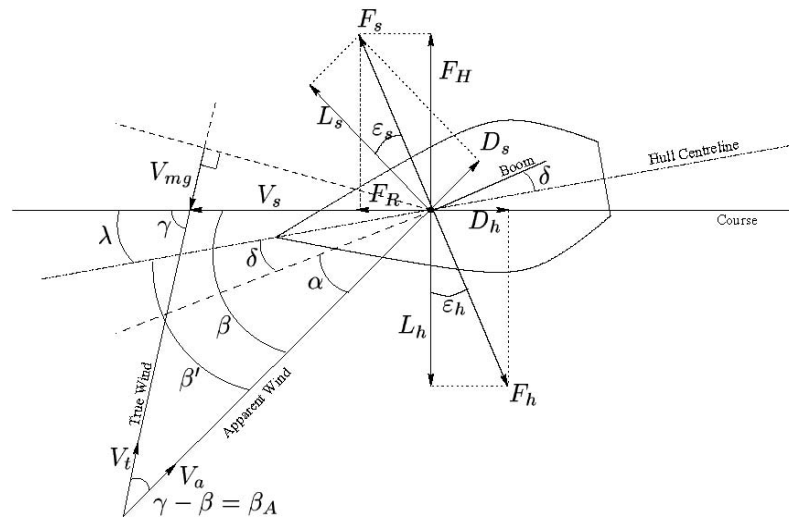


Fig. 2 Velocity vectors and forces acting on a boat in the sea-plane with heeling angle $\theta = 0$ (see Fig.3(a) for more details)

Once both models (2D-rigid and 3D-flexible) have been implemented the deflected shape of the sail has been used to derive a thickness fiber configuration (Part 3 in Fig. 1) over all the sail for a given wind speed and direction under a fixed strength criteria and constraint requirements. A number of numerical examples are also given to show the accuracy of the proposed method and comparisons with well-defined and established tests, belonging to the latest technical literature available (Bendsøe 1996), in order to validate the procedure.

2. Yacht mathematical formulation: velocities and forces on hull and sail

As the aero/hydro-dynamics of yacht sails is complex, it is essential to begin by focusing elementary background theory of sail aerodynamics and hull hydrodynamics. In turn, a first understanding of the overall equilibrium of forces and moments on a yacht (Marchaj 1990 and Claughton *et al.* 1998) is required. Fig. 2 illustrates the hull of a yacht sailing upright at a constant speed with the centre of effort (CE) of the sail and the centre of lateral resistance (CLR) of the submerged hull coincident. In Fig. 2 we use the following notations regarding velocity field: V_{mg} speed made good to windward or velocity made good; V_t wind velocity that can be measured by an observer fixed with respect to the sea (the speed made good V_{mg} is the component of the boat speed which is directly opposite to the true wind); V_a apparent wind velocity that can be directly measured on board (the apparent wind felt by sails varies in strength and direction over the mast height h , even if the true wind is steady (Fig. 3(c)); V_s boat speed through the water; is the speed of the boat with respect to the water. According to Fig. 2 we define the following notations for the angles: λ leeway angle; β angle between apparent wind and course or course angle, it is a measure of how high the boat is pointing (Claughton *et al.* 1998); $\beta' = \beta - \lambda$ apparent wind

angle between apparent wind and heading (angle measured by on-board instruments); γ angle between true wind and course or true wind angle; δ sheeting angle or angle between boom and centerline; α angle of incidence of wind on the sail or geometric angle of attack. The geometrical relationships between the six quantities, apparent wind speed V_a , apparent wind angle β , boat speed V_s , true wind speed V_t , true wind angle γ and speed made good to windward V_{mg} are fundamental and applicable to any boat on any point of sailing.

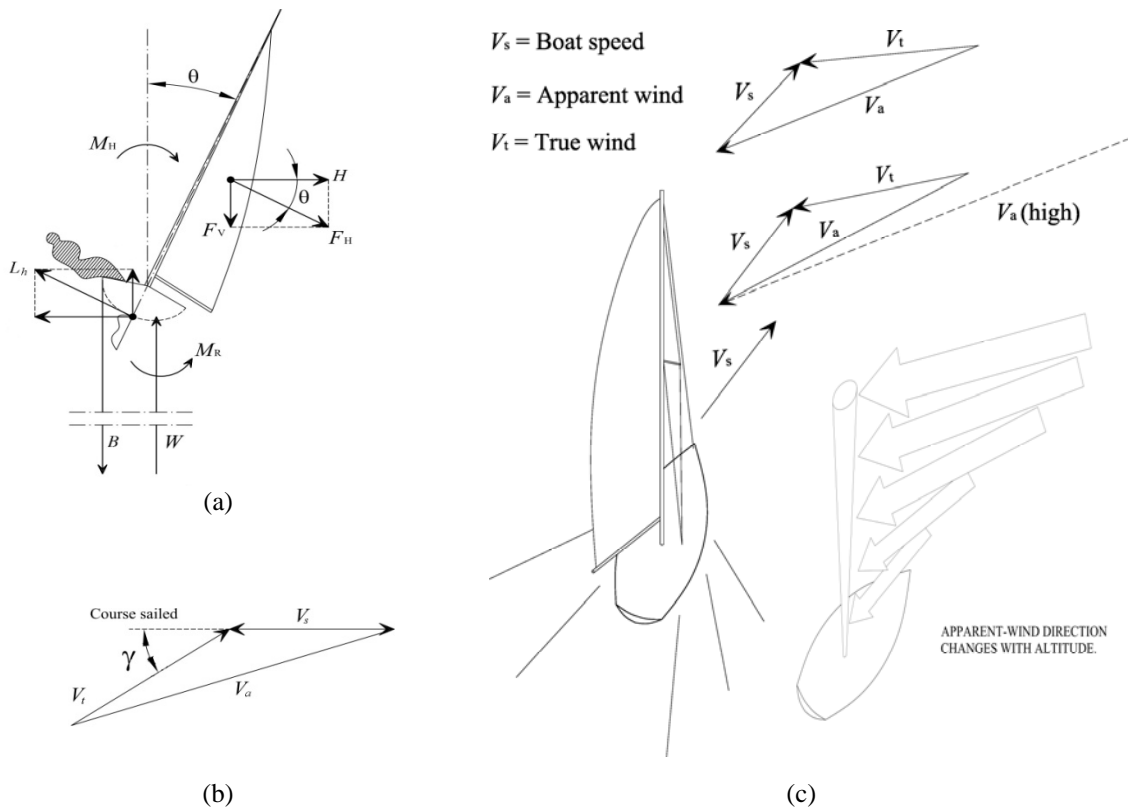


Fig. 3 Fundamental equilibrium equations of forces and moments acting on a sailboat system in a close-hauled steady-state condition (after Claughton *et al.* 1998, Whidden and Levitt 1990).

Even without any reference to the details of hull and sail characteristics, these relationships prescribe severe restrictions on the range of possible optimal performance of a sailboat against the wind. The following useful formulae are simply algebraic statements of the geometry of Figs. 2 and 3(a)

$$V_{mg} = V_s \cos \gamma \tag{1}$$

$$V_t \sin \gamma = V_a \sin \beta \quad (2)$$

$$V_s \sin \gamma = V_a \sin(\gamma - \beta) \quad (3)$$

$$(V_t + V_{mg})^2 + (V_{mg} \tan \gamma)^2 = V_a^2 = (V_s + V_t \cos \gamma)^2 + (V_t \sin \gamma)^2 \quad (4)$$

The previously defined simplification CE=CLR do not affect the geometrical relationships (1)-(4) (Marchaj 1990). From Eq. (4) we can derive the following relation

$$\frac{V_t}{V_a} = -\frac{V_{mg}}{V_a} + \sqrt{1 - \left(\frac{V_{mg}}{V_a} \tan \gamma\right)^2} \quad (5)$$

According to Figs. 2 and 3(a) we introduce the following notations in order to describe forces acting on the yacht system: forces on the hull like F_h (total hull force), L_h hull lift force perpendicular to fluid (water) flow direction, D_h hull drag force along fluid (water) flow direction; and forces on the sail: F_s total sail force or driving force (it can be resolved into two components (L_s , D_s) in a plane passing through the CE, as shown in Fig. 2), L_s sail lift force perpendicular to fluid (apparent wind air) flow direction, D_s sail drag force along fluid (apparent wind air) flow direction, F_R driving force of sails along course direction or propulsion or thrust force, F_H heeling force of sails acting perpendicular to both the course and the mast. This last force can be further resolved into two components, whose magnitudes will depend on the angle of heel θ (see Fig. 3(a)): $H = F_H \cos \theta$ (lateral sideforce in horizontal plane) and $F_V = F_H \sin \theta$ (vertical force of sail). When beating against the wind, we should like to have the maximum possible driving force F_R and simultaneously a minimum heeling force F_H so that we may sail at high speed with negligible heel and drift. From the following equilibrium relationships the magnitudes of F_R and F_H depend on angle β between the course and the apparent wind, and on lift L_s and drag D_s , that are assumed to act normal to the centre-plane of the hull and mast

$$F_R = L_s \sin \beta - D_s \cos \beta \quad (6)$$

$$H = F_H \cos \theta = (L_s \cos \beta + D_s \sin \beta) \cos \theta \quad (7)$$

From relations (6) and (7) the drag not only decreases the driving force F_R (Eq. (6)), but also increases the harmful heeling force F_H (Eq. (7)). It is not difficult to see that if the aerodynamic force on the sail, F_s , and the hydrodynamic force on the hull, F_h , are equal and opposite, as shown in Fig. 2, then the components of these forces, if taken along the same directions, must also be equal and opposite. This is shown in Fig. 2 where F_R is the component of F_s along the course sailed, for this reason it is called the driving force of the sails. This is exactly opposed by the hull drag force D_h measured along the direction of undisturbed water flow, which is simply

the direction of the course sailed. At right angles to these are the two independent force components F_H and L_h which are also equal and opposite. They are at right angles to the boat's direction of motion and so do not contribute to its speed but only to its tendency to heel.

As well as forces the boat is subject to torques or moments (Fig. 3(a)). If the boat is sailing with a constant angle of heel θ , the clockwise torque or heeling moment M_H produced by F_H and L_h must be exactly opposed by a counter clockwise moment, or righting moment M_R , produced by W , the total weight of the boat plus crew and B , the buoyancy force resulting from the displaced water (see Fig. 3(a)). Obviously W and B are equal and opposite, otherwise the boat would either rise up out of the water or sink farther into it.

3. Optimization of aero/hydro dynamic properties: mainsail windward performance

As highlighted in previous Section 2, the global analysis of sailboats requires understanding of complex interactions among aerodynamic and hydrodynamic forces and moments and structural stresses. It is possible to fully approach the complex problem (Parolini and Quarteroni 2005), but in this first part of the research a simplified numerical model has been selected able to reveal the skeletal form-shape of the sail (Part 1 in Fig. 1). It has been assumed the following main hypotheses (Sugimoto 1992, 1995):

1. the air is steady, inviscid and incompressible and the optimization of the performance of the sail has been done in light winds;
2. following from hypothesis 1 it has been neglected the effect of the boundary layer on water surface waves. The consequence is that the sea surface is assumed flat;
3. according to Section 2, regarding the driving force F_s created by the relative motion between sail and air, it is important that the drag resistance D_s be small. This is composed of induced drag, friction drag, form drag and additional resistance of rigging. Here it has been focusing only on induced drag so that $D_i \approx D_s$;
4. the sail has been designed to trim at zero heel angle $\theta = 0$ and the flexibility of the sail has been neglected; it will result in a flat rigid two-dimensional sail (Lasher *et al.* 2005). The effect of the hull is neglected. The flow around the sail will be affected by the close proximity of the sea and the presence of the hull, but if the latter entirely disappear, a reasonable estimation of the sea effect when the sail is in vertical attitude ($\theta = 0$) can be made by assuming that the surface acts as a reflecting plane so that an exact image of the sail appears below the surface (Marchaj 1990);
5. the yacht races are simply a series of windward and leeward legs as shown in Fig. 4(a). Because the most important performance of a yacht is its ability to sail to windward, it has been studied a single mainsail assumed to be close-hauled (Fig. 4(b)) (Lasher *et al.* 2005).

To summarize: it has been considered a single flat rigid mainsail assumed to be set close-hauled in uniform wind and upright on the flat sea surface. The ability of a yacht to sail to windward can be estimated by the speed made good V_{mg} which should be a maximum at each true wind velocity V_t (Eq. (5) and Figs. 3(b)-3(c)) (Fallow 1996, Doyle 2002). Whatever the hull form and rig size, the boat will sail in its most efficient mode in correspondence to the largest V_{mg} attained by larger V_s and smaller γ (Eq. (1)): an improvement of less than 0.5% in the velocity results in savings of around 25-35 seconds, which can be considered usually a margin of victory in a race

(Shankaran 2003).

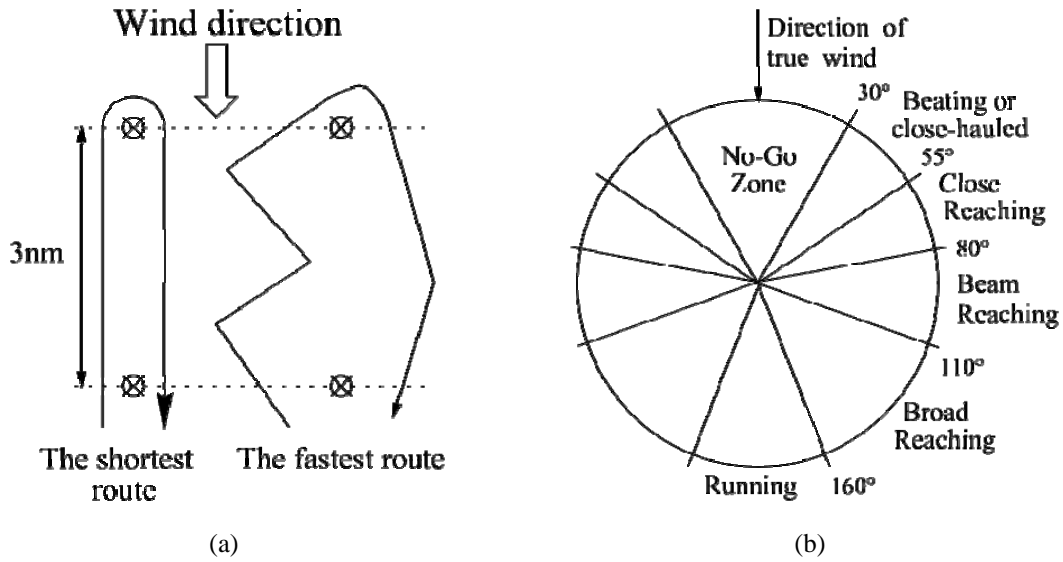


Fig. 4 Wind flow direction and points of mainsail

How can we obtain in our sail-boat system the largest V_s and smaller γ ? By following the considerations expressed below:

- i. the main objective function will be the thrust force F_R that must be maximized

$$V_s \cos \gamma \approx \sqrt{F_R} \cos \gamma \tag{8}$$

since the square of V_s is in direct proportion to the thrust force in steady-state sailing (Hypotheses 1), hence the largest V_s is obtained by maximizing F_R . But this is not enough, because it is evident that aerodynamic and hydrodynamic forces and moments have their maxima, but we need to consider that the lift L_s and the heeling moment M_H must be constrained;

- ii. in a steady state close-hauled sailing (Hypotheses 1 and 5) with $\theta = 0$ (Hypothesis 4) aerodynamic and hydrodynamic forces are in equilibrium; moving from Eqs. (6) and (7) we derive

$$\text{Hydro} \left\{ \begin{array}{l} D_h = \overbrace{L_s \sin \beta - D_s \cos \beta}^{F_R \text{ Aero}} \\ L_h = \overbrace{L_s \cos \beta + D_s \sin \beta}^{F_H \text{ Aero}} \end{array} \right. \underset{\text{Hypothesis 3}}{\approx} \begin{array}{l} L_s \sin \beta - D_i \cos \beta \\ L_s \cos \beta + D_i \sin \beta \end{array} \underset{\text{Hypothesis 5}}{\approx} \begin{array}{l} L_s \beta - D_i \\ L_s + D_i \beta \end{array} \tag{9}$$

Furthermore according to the conventional wing theory D_h can be approximated as a quadratic function of L_h and this resolve into $L_h \approx L_s + D_i\beta \approx L_s$. Therefore D_h reaches its maximum as L_h reaches its maximum and also as L_s reaches its maximum (Fallow 1996);

iii. the heeling bending moment M_H at the mast roof must be in equilibrium with the righting moment M_R produced by helms-men’s weights and by the weights of the boat and must be less than or equal the flexural strength moment M_m of the mast (Fig. 3(a)). Hence the righting moment has its upper limit. Therefore, either the mast strength or, better, the righting moment constraints the heeling moment.

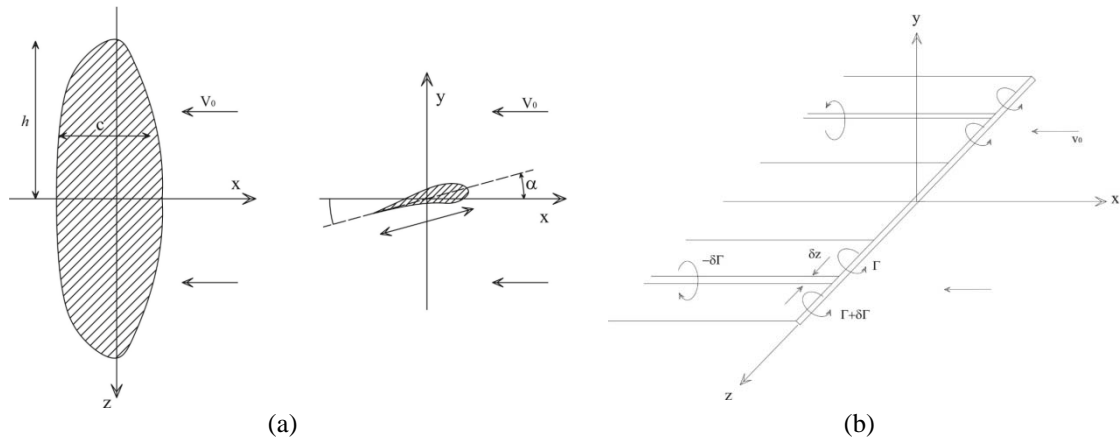


Fig. 5 (a) Lifting line theory: coordinate system and geometrical notation ($\alpha = \alpha_{ef} + \alpha_i$) to be used for a wing/sail and (b) trailing vortex system from a lifting line

To summarize, our design goal is the maximization of the aerodynamic thrust F_R via the optimal design of the sail, under the equality constraint on the lift L_s and the heeling moment $M_H (\leq M_m)$ due to stability problem and achieved imposing also the constraint on the mast height ($h = 3c$) and boom length or foot of the sail (c). Once the design goal concept is established it will be described numerically following the approach described by Sugimoto (1992, 1996) using the following dimensional quantities

$$L_s = \rho V_a^2 h^2 \int_{\delta}^1 \tilde{\gamma}(z) dz \tag{10}$$

$$M_H = \rho V_a^2 h^3 \int_{\delta}^1 [\tilde{\gamma}(z) \cos \beta + \tilde{\gamma}(z) \alpha_i(z) \sin \beta] z dz \approx \rho V_a^2 h^3 \int_{\delta}^1 \tilde{\gamma}(z) z dz \leq M_m \tag{11}$$

$$F_R = L_s \beta - D_i \tag{12}$$

$$D_i = \rho V_a^2 h^2 \int_{\tilde{\delta}}^1 \tilde{\gamma}(z) \alpha_i(z) dz \tag{13}$$

where h is the height of the mast, $\tilde{\delta}$ is a dimensionless gap between the sail foot and the sea surface and $z = Z/h$ is the dimensionless mast-coordinate axis. A sail behave like a thin wing at a certain angle of attack. Fig. 5 shows the coordinate system and notation to be used in case of a wing (or sail) assumed symmetrical about the central vertical plane on which $Z = 0$. The chord C , the geometrical angle of incidence α between the chord line and the main direction of the wing, and the cross-sectional shape (thickness) may all vary with the spanwise coordinate Z . The relevant property of the lifting line in Fig. 5(b) is the circulation Γ around a circuit enclosing the wing in a plane normal to the Z -axis. The lifting line theory is used to define the dimensionless circulation $\tilde{\gamma}(z)$ in Eqs. (10)-(13)

$$\tilde{\gamma}(z) = \frac{\Gamma(z)}{V_a h} \tag{14}$$

The induced angle of attack $\alpha_i(z)$ in Eqs. (11) and (13) represents the reduction of the effective incidence ($\alpha_{ef} = \alpha - \alpha_i$, where α is depicted in Fig. 5(a)) induced by circulation Γ and is given by

$$\alpha_i(z) = -\frac{1}{4\pi} \int_{\tilde{\delta}}^1 \frac{d\tilde{\gamma}(\zeta)}{d\zeta} \left(\frac{1}{\zeta - z} + \frac{1}{\zeta + z} \right) d\zeta \tag{15}$$

In order to simplify the numerical procedure, Eqs. (10)-(12) will be rewritten in a dimensionless form

$$L_{\max} = \int_{\tilde{\delta}}^1 \tilde{\gamma}(z) dz \tag{16}$$

$$M_{\max} \geq \int_{\tilde{\delta}}^1 \tilde{\gamma}(z) z dz \quad \Rightarrow \quad M_{\max} - \int_{\tilde{\delta}}^1 \tilde{\gamma}(z) z dz - \xi^2 = 0 \tag{17}$$

$$F_R = \int_{\tilde{\delta}}^1 \tilde{\gamma}(z) [\beta - \alpha_i(z)] dz \tag{18}$$

Using a slack variable ξ (Fletcher 1987), Eq. (17) has been written as an equality constraint (Venini and Nascimbene 2003). By introducing the following three Lagrange multipliers, corresponding respectively to the three Eqs. (16)-(18), λ_L , λ_M and λ_α , it is possible to write the problem as a maximization of the following functional (Sugimoto 1992, 1996)

$$\int_{\delta}^1 \left\{ \tilde{\gamma}(z) [\beta - \alpha_i(z)] + \lambda_a \left[\alpha_i(z) + \frac{1}{4\pi} \int_{\delta}^1 \frac{d\tilde{\gamma}(z)}{dz} \left(\frac{1}{\zeta - z} + \frac{1}{\zeta + z} \right) d\zeta \right] \right\} dz + \lambda_L \left(L_{\max} - \int_{\delta}^1 \tilde{\gamma}(z) dz \right) + \lambda_M \left(M_{\max} - \int_{\delta}^1 \tilde{\gamma}(z) z dz - \xi^2 \right) \quad (19)$$

The numerical solution of the functional (19), under the constraints on the strength mast moment M_m and on the mast height $h = 3c$, has been shown in Fig. 6 and compared with the 3DL mainsail from (Spalatelu-Lazar *et al.* 2008) (with $h = 2.2c$), the New Zealand mainsail from (Fallow 1996), the triangular and elliptical solution (with $h = 2c$) and the shape obtained by Sugimoto (1992, 1996). The numerical optimization process results in making a sail less “triangular” and more close to the “elliptical” form (Fallow 1996) which means less D_i when sailing upwind. The analyzed mainsail has an height of 30 m and a base of 10 m and has a geometrical dimensions which satisfies the proportion 3 to 1: height of the mainsail is three times greater than the base of the sail itself.

4. Optimization of mechanical properties: thickness and yarn layout

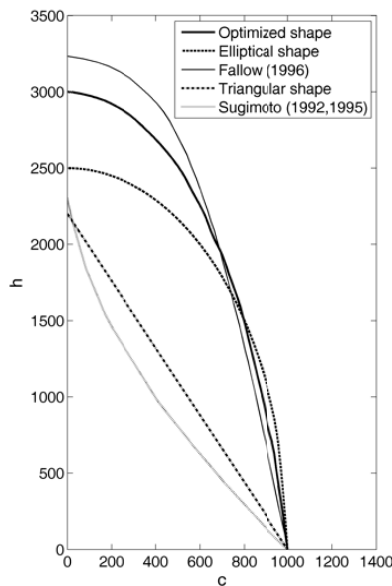


Fig. 6 Comparison of the optimized sail shape result (Part 1 Fig. 1) with more different configurations

Pressure distribution of the wind changes constantly and is affected by the shape of the sail, while the shape itself, through cloth stretch, strength and flexing, is affected by the pressure distribution of the wind. It is clear to understand that the properties of the cloth (warp, fill and bias,

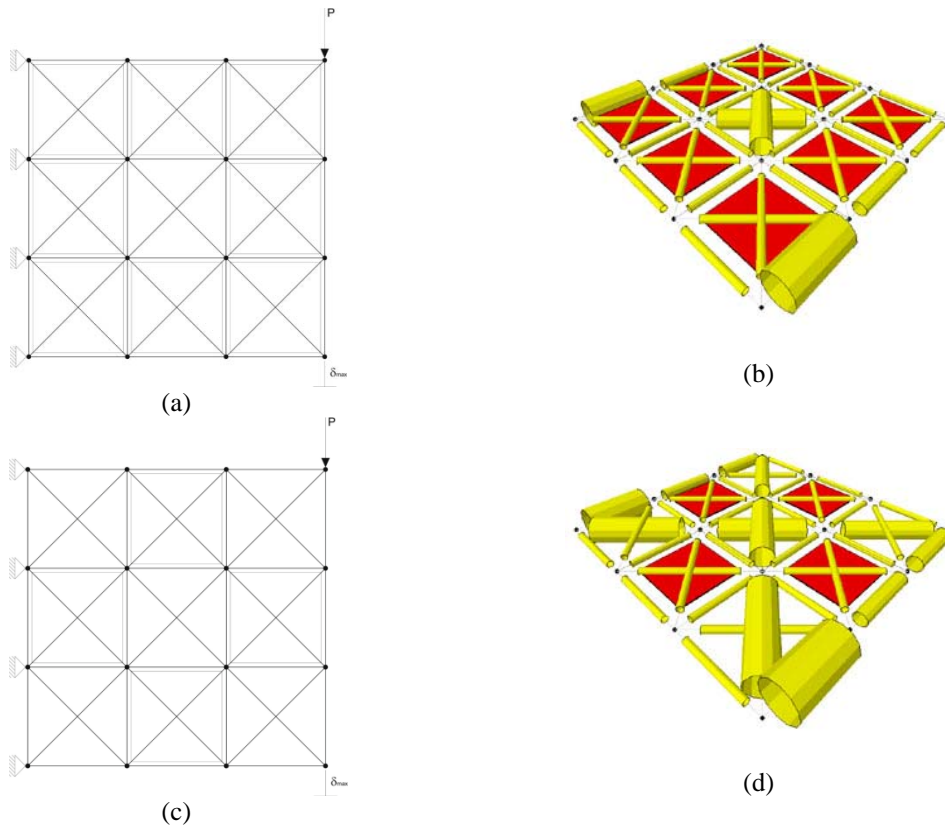
stretch resistance, strength, weight) play an important role in balancing aerodynamic forces and in shaping the sail. Moving from the optimized single mainsail assumed to be set close-hauled in uniform wind (Part 1 of the optimization process in Fig. 1 and optimized sail in Fig. 6), in order to take care of the mechanical properties of the cloth, we need to remove from our numerical model Hypothesis 4 by considering a flexible sail (no more rigid) able to undergo three-dimensional deformed configurations (no more flat). To this configuration we will apply separately Parts 2 (yarn orientation) and 3 (yarn thickness) of the flowchart in Fig. 1. In spite of the growing importance of textile composite materials (Tan *et al.* 1997), there is no systematic tool that can help to optimize its design while satisfying a set of target properties and imposed constraints. The designer of a textile composite material seeks to identify the best fiber and matrix thickness, the most appropriate fiber preform structure and different yarn volume fractions. Optimum design of textile composites, or even its estimation thereof is important for the following reasons: to reduce expenses involved in trial and error procedures, to open grounds for possible new fabric designs able to deliver a set of unique target properties, to obtain the best performance of a material in an application and to identify a cost-effective design.

Aim of our formulation is to integrate a finite element computational code, used to model the membrane-matrix and the fiber distribution, with an appropriate optimization method. In this approach the finite element model is used as an analysis tool to evaluate structural responses (i.e., displacements, strains and stresses) and their sensitivities with respect to design variables under the given loading conditions (wind); the optimization routine is an iterative optimization algorithm aimed to find improved feasible designs with the knowledge of structural responses and sensitivity information, obtained by the finite element procedure. Due to the implicit relationship between structural responses and design variables, the optimization strategy usually called Sequential Convex Programming (SCP) is used to replace approximately the original problem by solving a sequence of explicit and convex sub-problems (Svanberg (1987)). An up-to-date review of optimization methods and applications can be found in Bendsøe and Sigmund (2003).

4.1 Complete model: reliability test

To confirm the reliability of the method here proposed and applied to a composite sail, we will present a few examples regarding full optimization of simple structures composed of membrane and arch finite elements (i.e., made of matrix and fiber). This constitutes the final and definitive step that gives us the possibility to model the sail behavior under a generic wind-load-pressure distribution. Let us consider the structures presented in Figs. 7(a) and 7(c). The results, obtained asking for the optimum design of the fiber sectional area under displacement constraints, are depicted in Figs. 7(b) and 7(d): in the void zones all the stress field due to the applied load is taken and adsorbed by the fibers because the collaboration of the membrane material is absent. The optimized section distribution “compels” the arch elements to assume a bigger area in the part of the structure where there is no collaboration between membrane and fibers. The last example to test the reliability of the procedure in the case of simultaneous presence of membrane and arch finite elements is represented by the case of a pinched beam (Fig. 8(a)). In spite of a very poor mesh (Fig. 8(b)) we can note the classical “candy” configuration assumed by the optimized structure in which the fibers have greater areas in the same zones where in the previous case the membranes have the greater thicknesses. It is important to clarify that the proposed model does not explicitly take into account buckling phenomena due to fiber compression, because sail

optimization does not require such a capability.



Figs. 7 (a)-(c) Starting geometries and (b)-(d) optimized results in two cases of membrane meshes with and without holes: (a) central hole and (c) symmetric holes

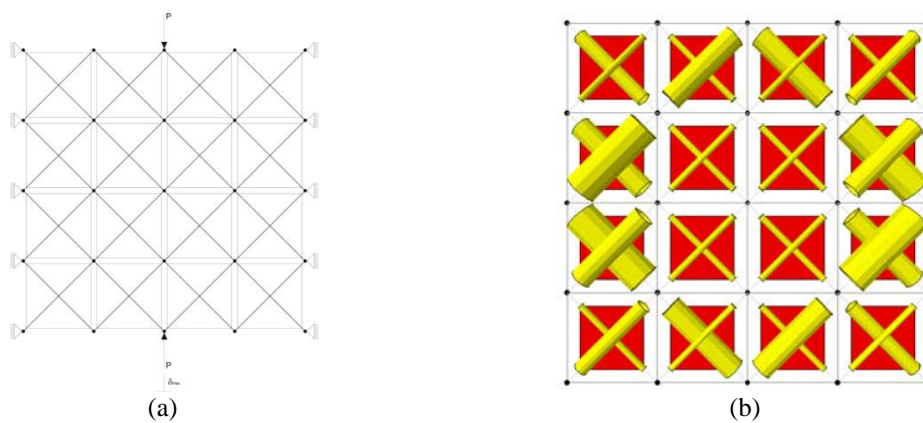


Fig. 8 Problem statement: pinched beam with membrane and truss elements: (a) geometrical configuration and (b) optimal sectional area distribution

4.2 Real mainsail optimization result: orientation and thickness distribution against the wind

A modern sail for boats is made by a composition of matricial component of the fiber-reinforced material, modeled by membrane finite elements, and reinforcing fibers modeled by arch-type finite elements (Nascimbene 2012). In opposition to the most recent and advanced theories proposed in the last decade for the investigation of the structural behavior of sails, see for more details (Tabiei and Ivanov 2003, Charvet *et al.* 1996), in our theory we have decided to consider at the same time both the fibrous and the matricial component using a unique mesh to model the sail. The optimization process is based on the study of a discretized sail composed by membrane and arch finite elements. In the first Part 1 (Fig. 1) of the iterative process described in Sections 2 and 3, a flat 2D sail has been obtained and depicted in Fig. 6. Moving from the undeformed and unstressed optimized rigid sail, a 3D flexible structure has been derived. It has been discretized by membrane elements and loaded by a pressure wind distribution over the mast height h . From the finite element model it has been obtained the stress distribution in the sail providing also the exact configuration of the isostress lines all along the flexible surface. Following this distribution, the numerical algorithm is able to re-orient the membrane mesh putting a new network made of arch finite elements on the new distorted mesh, assuring that each curve element have the two nodal points belonging to two nodal points of the membrane quadrangular element and that the arch local axis correspond to the side of the membrane element itself.

Only at this point the optimization process can start: taken orientation and membrane thickness as fixed, the procedure looks for the optimal distribution of the cross section areas of the fiber elements, whose optimal geometric configuration has been determined at the previous step. The different steps by which the optimization of a fiber-matrix sail has been performed are resumed in the next points:

- Step 1 (starting step): the optimized shape sail obtained in Section 3 and depicted in Fig. 6 is the starting point. In order to obtain numerically the 2D optimized shape a number of five main hypotheses have been highlighted in Section 3. A few of them can be removed due to the fact that the sail will be considered in a 3D flexible/deformed configuration loaded by a wind distribution. According to Fig. 3 the air distribution acting on the 3D sail main be modeled using the following logarithmic profile (Hedges *et al.* 1996)

$$V_t = \frac{\bar{u}}{K} \ln \left(1 + \frac{Z}{Z_0} \right) \quad (20)$$

where K , assumed equal to 0.4, is the von Karman's constant, Z_0 the surface roughness length (in case of moderate wind condition $Z_0 = 0.001$ m) and \bar{u} the friction velocity;

- Step 2: all the geometrical and mechanical properties for the matrix and composite fibers are known (Kevlar Mylar material). Using the classical finite element techniques, the matrix component of the structure is discretized in N_e quadrilateral membrane finite elements with four nodes. Geometrically nonlinear membrane model with zero flexural stiffness, described by Contri

and Schrefler (1988), has been used within the total lagrangian framework;

- Step 3: performs a first finite element analysis of the sail-membrane structure (using a displacement-based approach), producing nodal displacements of discretized structure and stress field at the Gauss-points as output;

- Step 4: calculates the distribution of the isostress lines (Part 2 in Fig. 1) used to deform the computational mesh. Some dedicated subroutines can now mark in a special way the side nodes of the finite element discretization of the structure by writing the history of the fiber angle for each element. While the side nodes determined at the previous Steps 2 and 3 remain fixed in their original geometrical position (i.e., mast and boom) in the finite element discretization, the mesh of the structure is re-oriented in order to obtain a “deformed” and “distorted” mesh in which every side of the single finite element tries to follow the global distribution of the isostress lines. One of the most severe constraint to respect during the re-orientation process is constituted by the geometrical continuity of the mesh: we thus have to ensure that no holes can be present in the new re-oriented mesh and that the right nodal connectivity system is maintained also in the final distorted configuration. The approach to update fiber orientation follows the formulation in reported by Tabiei and Ivanov (2003). Cheng and Kikuchi (1994) as well as Pedersen (1989) must be considered as pioneering contributions in the optimal design of fiber orientation for composite structures;

- Step 5: over the new re-oriented mesh we can now put a three-dimensional network realized by arch finite elements that represent the fiber component of the composite material: in this way, these rope finite elements follow the isostress lines calculated before. The element must be able to avoid membrane and shear locking and violent stress oscillations in the thin limit (Nascimbene 2012, DellaCroce *et al.* 2003, Nascimbene and Venini 2002). The main features of this element lies in the Based Gauss Mixed Interpolation (BGMI) of the normal/tangential generalized displacements and of the strains. Bruggi (2008) and Bruggi and Venini (2007) are among the few adopting mixed elements in topology optimization. Very recently the fabrication technology, usually called 3DL, allows to arrange the fiber layout according to a curvilinear path all along the sail surface. This types of fabrication, in order to be rightly modeled, requires a arch curvilinear very thin finite element such as the one proposed by Nascimbene (2012);

- Step 6: performs a new geometrically non linear finite element analysis of the complete structure, now made of both membrane and rope elements (representing respectively the matrix and the fiber parts of the composite; Part 3 in Fig. 1);

- Step 7: runs an optimization step and performs pre numerical sensitivity analysis of the problem. Particularly a failure analysis on maximum stress at any point must be verified. The failure criterion is based on the evaluation of the maximum stress in the principal coordinates compared to the respective strength;

- Step 8: if the optimum condition is reached, then gives an output in which the optimal values assumed by the objective function and by every single design variable at the optimum design point are presented; conversely, the optimization loop returns to Step 3 in order to perform a new analysis with new values for the design variables.

According to Part 2 in Fig. 1 we have first analyzed the problem of the optimal orientation for the reinforcing fibers included into a typical modern competition sail, as that one optimized and illustrated in Fig. 6. We have considered (Fig. 9(a)) a quadrangular finite element mesh for the mainsail using 400 membrane quadrangular finite elements, modeling the matricial part of fiber-reinforced composite material by which the sail is made of. In Fig. 9(b) the global isostress lines configuration in every single quadrangular membrane finite element is represented, while the other four images (Fig. 10) represent several zoomed in figures for different parts of the sail to show in a better way the real stress distribution. We want to remember that the length of every single line inside the quadrangular finite element is proportional to the intensity value of the measured stress in that element. The most intense stress values are concentrated near the top of the mainsail. Once the procedure has determined isostress line configuration inside the mainsail, we can finally try to re-orient the mesh, following the prescriptions provided at Step 4 above. Note that it is very important not to alterate the spatial coordinates of the side nodes of the mesh that define the real shape of the sail. Moving also these nodes would destroy the original geometrical definition of sail shape, obtained in Section 3 and depicted in Fig. 6, with the consequent loss of meaning for the starting point of the optimization problem (Part 1 in Fig. 1), losing in other word the physical definition of the problem itself.

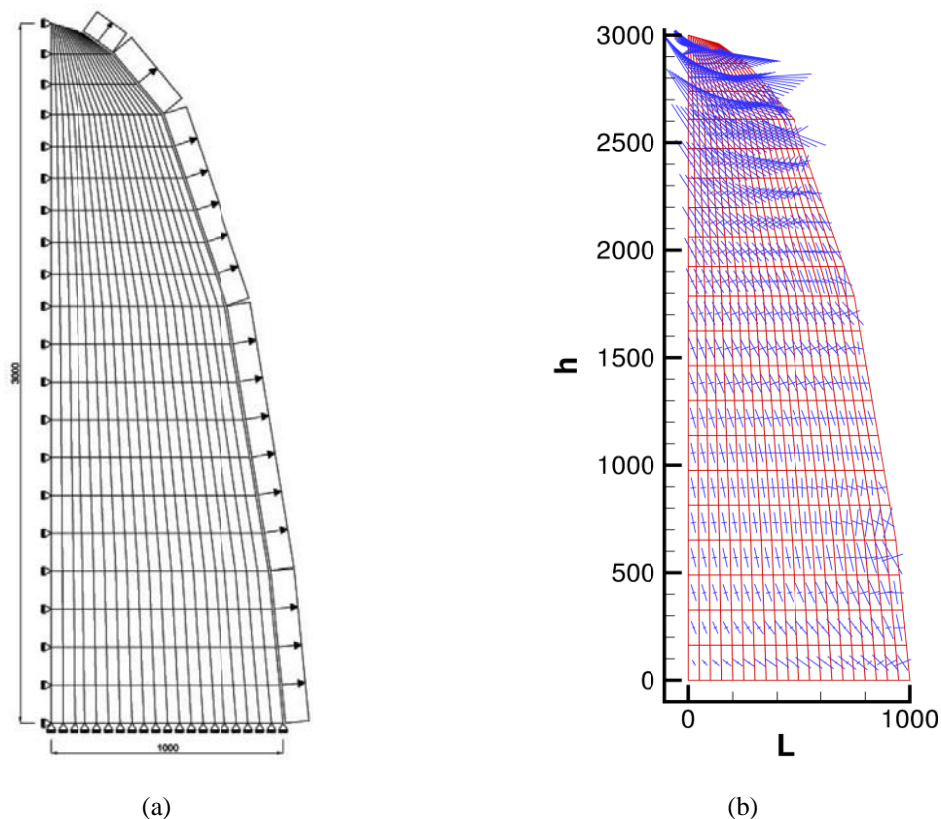


Fig. 9 (a) Modern competitor mainsail, discretized by a quadrangular finite element mesh and (b) global view for the isostress lines inside the mainsail

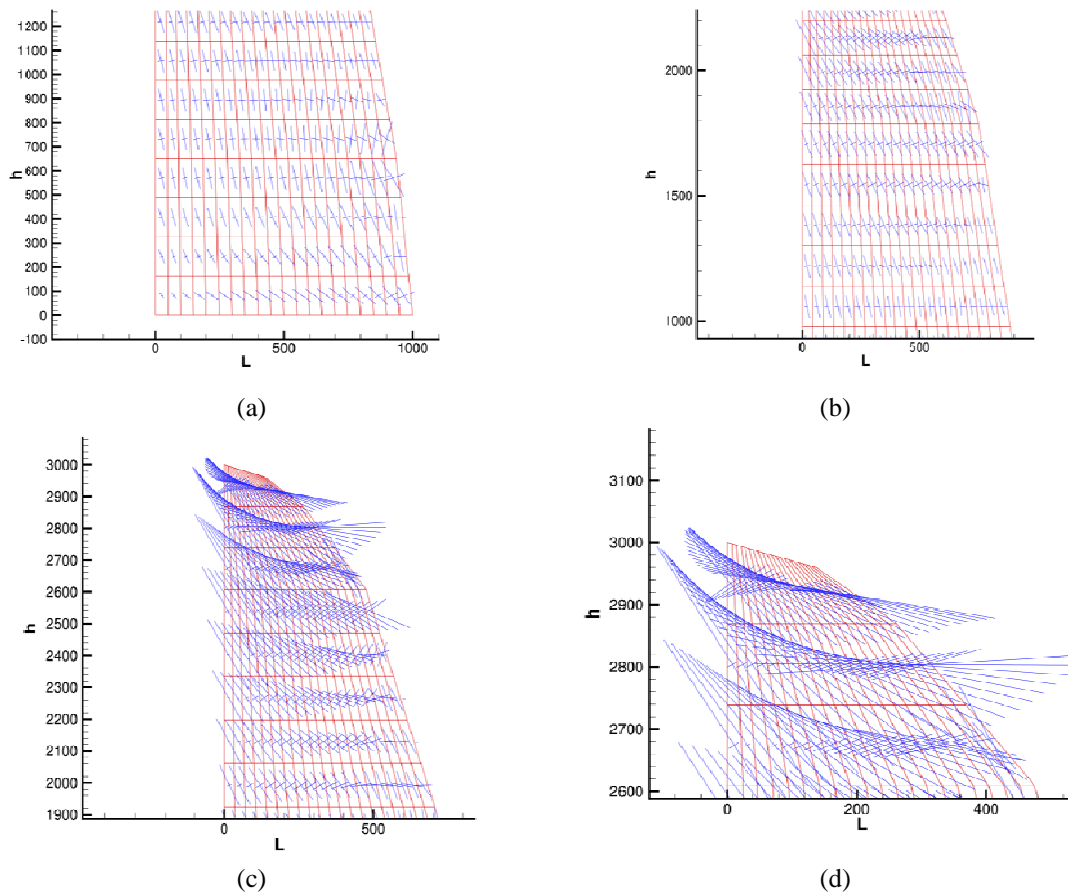


Fig. 10 (a) Boom of the mainsail, (b) boom and middle area of the mainsail, (c) middle area and top of the sail and (d) top of the sail

In Fig. 11 the graphical results of the re-orientation process are presented as performed by the procedure during the several convergence steps done in the iterative optimization process. We present the initial undeformed mesh configuration (Fig. 11(a)) and the final re-oriented mesh configuration, reached at the last step of the optimization problem (Fig. 11(b)). Fig. 11(c) presents the yarn layout that was put on the re-oriented mesh before to begin the final optimization problem (Part 3 in Fig. 1 and Steps 5-8 above) whose aim is to determine the optimal section area distribution of the fibers inside the sail. Close similarities with fiber layout presented by Fallow (1996) and Spalatelu-Lazar (2008) can be observed in Fig. 11(c): at the base of the mainsail on the left (tack) the optimal orientation is $30^\circ/40^\circ$, while on the right (clew) is $-30^\circ/-40^\circ$; close to the top of the mainsail (head) the most part of the fibers are oriented at $75^\circ-90^\circ$ while in the center of the sail surface the fibers are principally oriented at $-10^\circ/0^\circ/10^\circ$.

The re-oriented mesh with the new final configuration of the reinforcing fibers is now optimized in the distribution of the fiber section area, producing the final graphical results

illustrated by Fig. 12, obtained supposing that the rate of fibers has a maximum of 90% at the top and in the corners of the sail and 60% elsewhere (Spalatelu-Lazar 2008).

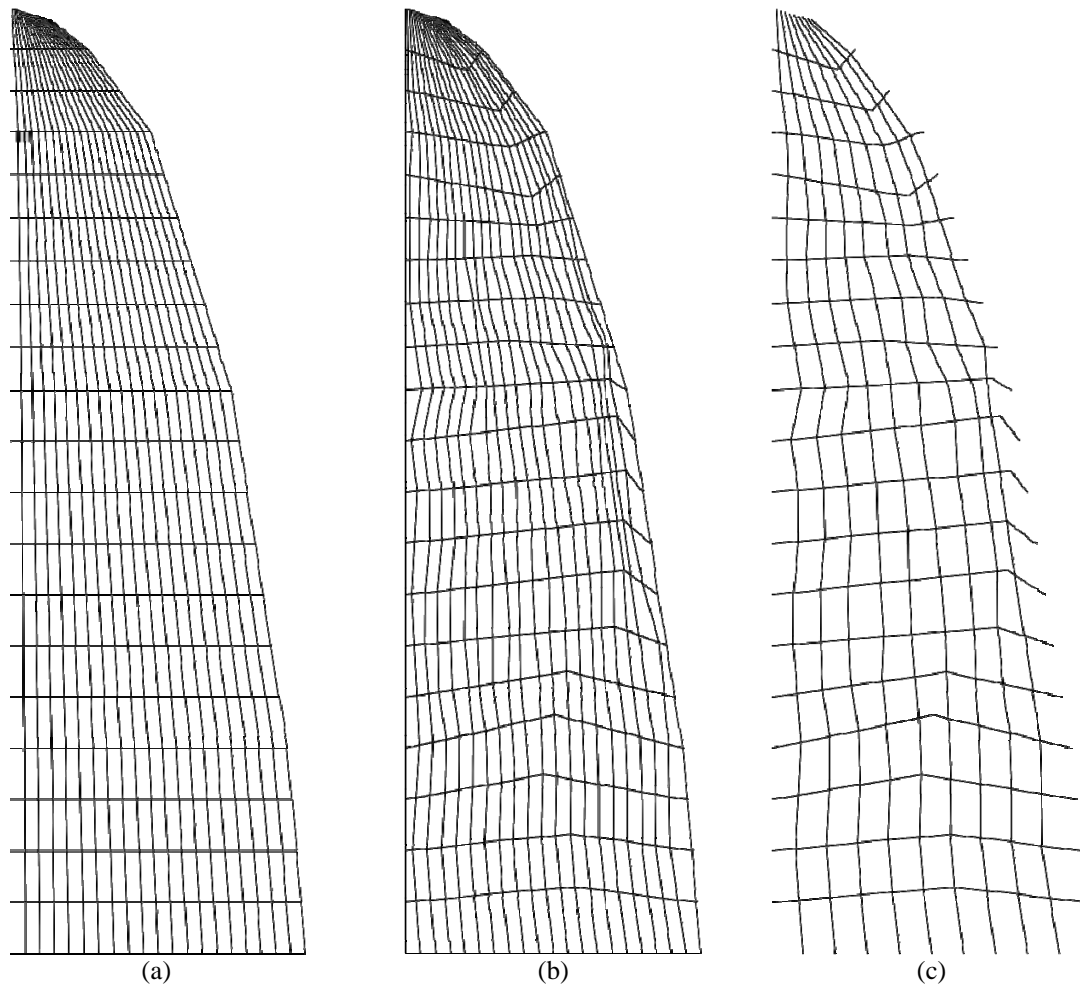


Fig. 11 (a) Initial original mesh configuration (undeformed), (b) final configuration of the mesh reorientation process and (c) truss-fibers network

In the last step of the optimization problem we have finally determined the optimal sectional area distribution for the reinforcing fibers inside the sail after that the optimal and more effective geometrical configuration of the fibers themselves was determined by the disposition of the truss net on the re-oriented mesh, whose border lines follow the isostress lines distribution. Fig. 12 depicts the optimized section area fibers distribution for a mainsail mesh realized by 400 membrane quadrangular finite elements, modeling the matricial part of fiber-reinforced composite material by which the sail is made of, and 760 arch finite elements, that represent the reinforcing fibers. We want to note that every single membrane finite element was surrounded by four arch

finite elements, one for each of the four sides of the quadrangular element.

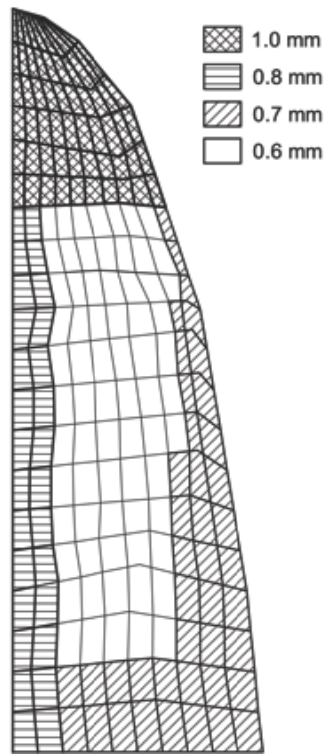


Fig. 12 Thickness optimization corresponding to yarn layout

5. Conclusions

A multiple criteria optimization tool for sail design, analysis and optimization has been described. Its application to real structural cases has been found to be reliable, robust and accurate. The yarn distribution and thickness affects the flexible real behavior of the sail membrane and requires a design development process in order to find the best possible solution. This is achieved in this research by starting from a simplified two dimensional flat undeformed model and then moving to a three dimensional flexible flying-shape sail, to account for the elastic nature of the sail cloth. Improved structural model of the mainsail is derived for a number of wind and regatta conditions. By using the multiple criteria developed in this research we were able to improve quality, efficiency and performance of a mainsails using analytical and numerical optimization procedures as well as advanced non linear finite element modeling.

Acknowledgments

This research derived originally from discussion among the author, Dr. Manuel Bergamaschi

when he was a student under my supervision at the Department of Structural Mechanics at the University of Pavia and Prof. Armando Gobetti. His guidance and suggestions are appreciated.

References

- Bendsøe, M.P. (1996), *Optimization of structural topology, shape, and material*, New York, Springer.
- Bendsøe, M.P. and Sigmund, O. (2003), *Topology Optimization - Theory, Methods and Applications*, Springer, Berlin.
- Bruggi, M. (2008), "On the solution of the checkerboard problem in mixed-FEM topology optimization", *Comput. Struct.*, **86**(19-20), 1819-1829.
- Bruggi, M. and Venini, P. (2007), "Topology optimization of incompressible media using mixed finite elements", *Comp. Meth. App. Mech. Eng.*, **196** (33-34), 3151-3164.
- Charvet, T., Hauville, F. and Huberson, S. (1996), "Numerical simulation of the flow over sails in real sailing conditions", *J. Wind Eng. Ind. Aerod.*, **63**(1-3), 111-129.
- Cheng, H.C. and Kikuchi, N. (1994), "An improved approach for determining the optimal orientation of orthotropic material", *Struct. Optim.*, **8**(2-3), 101-112.
- Cinquini, C., Venini, P., Nascimbene, R. and Tiano, A. (2001), "Design of a river-sea ship by optimization", *Struct. Multidiscip. O.*, **22**(3), 240-247.
- Claughton, A.R., Wellicome, J.F. and Sheno, R.A. (1998), *Sailing Yacht Design: Theory*, Edinburgh, Addison Wesley Longman Limited.
- Contri, P. and Schrefler, B.A. (1988), "A geometrically nonlinear finite element analysis of wrinkled membrane surface by a no-compression material model", *Commun. Numer. Meth. En.*, **4**(1), 5-15.
- DellaCroce, L., Venini, P. and Nascimbene, R. (2003), "Numerical Simulation of an Elastoplastic Plate via Mixed Finite Elements", *J. Eng. Math.*, **46**(1), 69-86.
- Doyle, T., Gerritsen, M. and Iaccarino, G. (2002), *Towards sail-shape optimization of a modern clipper ship*, Centre for Turbulence Research, Annual Research Briefs.
- Fallow, J.B. (1996), "America's Cup sail design", *J. Wind Eng. Ind. Aerod.*, **63**(1-3), 183-192.
- Fletcher, R. (1987), *Practical methods of optimization*, 2nd ed. London, John Wiley and Sons.
- Fleury, C. (1989), "CONLIN: an efficient dual optimizer based on convex approximation concepts", *Struct. Optim.*, **1**(2), 81-89.
- Hedges, K.L., Richards, P.J. and Mallison, G.D. (1996), "Computer modeling of downwind sails", *J. Wind Eng. Ind. Aerod.*, **63**, 95-110.
- Lasher, W.C., Sonnenmeier, J.R., Forsman, D.R. and Tomcho, J. (2005), "The aerodynamics of symmetric spinnakers", *J. Wind Eng. Ind. Aerod.*, **93**(4), 311-337.
- Marchaj, C.A. (1990), *Sail Performance: Techniques to maximize Sail Power*, Camden, International Marine.
- Moraes, H.B., Vasconcellos, J.M. and Almeida, P.M. (2007), "Multiple criteria optimization applied to high speed catamaran preliminary design", *Ocean Eng.*, **34**, 133-147.
- Nascimbene, R. (2013), "An arbitrary cross section, locking free shear-flexible curved beam finite element", *Int. J. Comp. Meth. Eng. Sci. Mech.*, **14**(2), 90-103.
- Nascimbene, R. and Venini, P. (2002), "A new locking-free equilibrium mixed element for plane elasticity with continuous displacement interpolation", *Comput. Method. Appl. M.*, **191**, 1843-1860.
- Parolini, N. and Quarteroni, A. (2005), "Mathematical models and numerical simulations for the America's Cup", *Comput. Method. Appl. M.*, **194**, 1001-1026.
- Pedersen, N. (1989), "On optimal orientation of orthotropic materials", *Struct. Optim.*, **1**, 101-106.
- Shankaran, S. (2003), *Numerical analysis and design of upwind sails*, Ph.D. Thesis, Stanford University.
- Spalatel-Lazar, M., Léné, F. and Turbé, N. (2008), "Modelling and optimization of sails", *Comput. Struct.*, **86**, 1486-1493.
- Sugimoto, T. (1992), "A first course in optimum design of yacht sails", *Proceedings of the 11th Australasian Fluid Mechanics Conference*, University of Tasmania, Hobart, Australia.
- Sugimoto, T. (1995), "Optimum sail design for small heel and weak wind shear conditions", *Fluid Dyn. Res.*,

- 15**(2), 75-88.
- Svanberg, K. (1987), "Method of moving asymptotes - A new method for structural optimization", *Int. J. Numer. Meth. Eng.*, **24**, 359-373.
- Tabiei, A. and Ivanov, I. (2003), "Fiber reorientation in laminated and woven composites for finite element simulations", *J. Thermoplast. Compos.*, **16**(5), 457-474.
- Tan, P., Tong, L. and Steven, G.P. (1997), "Modelling for predicting the mechanical properties of textile composites-a review", *Compos. Part A*, **28**(11), 903-922.
- Venini, P. and Nascimbene, R. (2003), "A new fixed-point algorithm for hardening plasticity based on nonlinear mixed variational inequalities", *Int. J. Numer. Meth. Eng.*, **57**(1), 83-102.
- Whidden, T. and Levitt, M. (1990), *The art and science of sails: A Guide to Modern Materials, Construction, Aerodynamics, Upkeep, and Use*, St. Martin's Press.